

Thermal conduction and particle transport in strong MHD turbulence, with application to galaxy-cluster plasmas

Benjamin D. G. Chandran

Department of Physics & Astronomy, University of Iowa

benjamin-chandran@uiowa.edu

Jason L. Maron

jason-maron@uiowa.edu

Department of Physics & Astronomy, University of Iowa, and Department of Physics & Astronomy, University of Rochester

ABSTRACT

Galaxy clusters possess turbulent magnetic fields with a dominant scale length $l_B \simeq 1 - 10$ kpc. In the static-magnetic-field approximation, the thermal conductivity κ_T for heat transport over distances $\gg l_B$ in clusters is $\simeq \kappa_S l_B / L_S(\rho_e)$, where κ_S is the Spitzer thermal conductivity for a non-magnetized plasma, the length $L_S(r_0)$ is a characteristic distance that a pair of field lines separated by a distance $r_0 < l_B$ at one location must be followed before they separate by a distance l_B , and ρ_e is the electron gyroradius. We introduce an analytic Fokker-Planck model and a numerical Monte Carlo model of field-line separation in strong magnetohydrodynamic (MHD) turbulence to calculate $L_S(r_0)$. We also determine $L_S(r_0)$ using direct numerical simulations of MHD turbulence with zero mean magnetic field. All three approaches, like earlier models, predict that L_S asymptotes to a value of order several l_B as r_0 is decreased towards l_d in the large- l_B/l_d limit, where l_d is the dissipation scale, which is taken to be the proton gyroradius. When the turbulence parameters used in the Fokker-Planck and Monte Carlo models are evaluated using direct numerical simulations, the Fokker-Planck model yields $L_S(\rho_e) \simeq 4.5l_B$ and the Monte Carlo model yields $L_S(\rho_e) \simeq 6.5l_B$ in the large- l_B/l_d limit. Extrapolating from our direct numerical simulations to the large- l_B/l_d limit, we find that $L_S(\rho_e) \simeq 5 - 10l_B$, implying that $\kappa_T \simeq 0.1\kappa_S - 0.2\kappa_S$ in galaxy clusters in the static-field approximation. We also discuss the phenomenology of thermal conduction and particle diffusion in the presence of time-varying turbulent magnetic fields. Under the questionable assumption that turbulent resistivity completely reconnects field lines on the time scale l_B/u , where u is the rms turbulent velocity, we find that κ_T is enhanced by a moderate amount relative to the static-field estimate for typical cluster conditions.

1. Introduction

In the cooling-flow (CF) model of intracluster plasma, radiative cooling causes plasma to flow towards a cluster’s center and cool to sub-x-ray temperatures, presumably ending up as either stars, smaller compact objects, and/or cold gas. Aside from the gravitational work done on inflowing plasma, heating of intracluster plasma is neglected in the model, and mass accretion rates \dot{M} are as high as $10^3 M_\odot \text{ yr}^{-1}$ for some clusters (Fabian 1994). A longstanding problem for the CF model has been the difficulty in accounting for all the accreted mass. For example, the observed rates of massive star formation are a factor of 10-100 less than expected if the cooling plasma predicted by the model ends up forming stars with a normal IMF (Crawford et al 1999, Fabian 2002). In addition, recent x-ray observations find no evidence of plasma cooling to temperatures below 1-2 keV (Peterson et al 2001, Tamura et al 2001). These difficulties suggest that some form of heating approximately balances radiative cooling, thereby dramatically reducing \dot{M} relative to CF estimates. A number of heating mechanisms have been considered, such as galaxy motions (Bregman & David 1989), supernovae (Bregman & David 1989), cosmic-rays (Bohringer & Morfill 1988, Tucker & Rosner 1983), active galactic nuclei (Pedlar et al 1990, Tabor & Binney 1993, Binney & Tabor 1995, Ciotti & Ostriker 2001, Churazov et al 2002), dissipation of turbulent energy (Loewenstein & Fabian 1990, Churazov et al 2003, Chandran 2003), and thermal conduction, which can transport heat from the hot outer regions of a cluster into the relatively cooler core (Binney & Cowie 1981, Tribble 1989, Tao 1995, Chandran & Cowley 1998, Narayan & Medvedev 2001, Gruzinov 2002, Voigt et al 2002, Zakamska & Narayan 2002). For thermal conduction to approximately balance cooling, the thermal conductivity κ_T must be a significant fraction of the Spitzer value for a non-magnetized plasma, κ_S , and in some clusters even greater than κ_S (Fabian 2002, Zakamska & Narayan 2002), where

$$\kappa_S = 5.2 \times 10^{32} \left(\frac{k_B T}{10 \text{ keV}} \right)^{5/2} \left(\frac{10^{-3} \text{ cm}^{-3}}{n_e} \right) \left(\frac{37}{\ln \Lambda} \right) \frac{\text{cm}^2}{\text{s}}, \quad (1)$$

T is the temperature, k_B is the Boltzmann constant, n_e is the electron density, and $\ln \Lambda$ is the Coulomb logarithm (Spitzer 1962).¹

Galaxy clusters are filled with tangled magnetic fields with a dominant length scale $l_B \simeq 1 - 10$ kpc (Kronberg 1994, Taylor et al 2001, 2002) that is much less than the size of a cluster core, $R_c \simeq 100$ kpc. Both optical-line-emitting gas in clusters and hot intracluster plasma are observed to be in turbulent motion (Fabian 1994, Churazov et al 2003). The effects of turbulent magnetic fields and velocities on κ_T are the subject of this paper, and have been investigated by a number of authors (e.g., Tribble 1989, Tao 1995, Chandran & Cowley 1998, Chandran et al 1999, Narayan & Medvedev 2001, Malyskin & Kulsrud 2001, Gruzinov 2002).

¹In terms of this definition, in which κ_S is expressed as a diffusion coefficient, the heat flux is given by $-n_e k_B \kappa_S \nabla T$.

Transport in the presence of strong turbulence is a difficult and unsolved problem. It is likely that the thermal conductivity for a particle species scales like the test-particle diffusion coefficient for that particle species (Rechester & Rosenbluth 1978, Krommes, Oberman, & Kleva 1983): since the collisional transfer of energy between particles occurs locally in space, diffusion of heat accompanies the diffusion of heat-carrying particles. We thus estimate κ_T in clusters from the relation

$$\frac{\kappa_T}{\kappa_S} \simeq \frac{D}{D_0}, \quad (2)$$

where D is the diffusion coefficient of thermal electrons and D_0 is the thermal-electron diffusion coefficient in a non-magnetized plasma.^{2 3 4}

Since thermal electrons in clusters move much faster than the $\mathbf{E} \times \mathbf{B}$ velocity of field lines, a reasonable first approximation for D is obtained by treating the magnetic field as static. In a collisional plasma, particle diffusion over distances $\gg l_B$ in a static field depends critically on the rate of separation of neighboring magnetic field lines (Rechester & Rosenbluth 1978, Chandran & Cowley 1998). If two field lines within a snapshot of strong magnetohydrodynamic (MHD) turbulence are at some location separated by a distance $r_0 \ll l_B$, they will separate by a distance l_B after some distance z along the magnetic field. The length $L_S(r_0)$ is a characteristic value of z defined in section 2. In the static-magnetic field approximation, the thermal conductivity κ_T in galaxy clusters over distances $\gg l_B$ satisfies

$$\kappa_T \simeq \frac{\kappa_S l_B}{L_S(\rho_e)}, \quad (3)$$

where ρ_e is the electron gyroradius. Equation (3) makes use of the fact that electron motion along the magnetic field is relatively unimpeded by magnetic mirrors and whistler waves excited by the heat flux because the Coulomb mean free path is short compared to both l_B and the temperature-gradient length scale (see section 3). The factor $l_B/L_S(\rho_e)$ in equation (3) measures the reduction in κ_T associated with tangled field lines, which increase the distance electrons must travel in going from hotter regions to colder regions.

²Electrons generally make the dominant contribution to κ_T because they diffuse more rapidly than ions.

³In a steady state, an electric field is set up to maintain quasi-neutrality. This electric field reduces κ_T by a factor of $\simeq 0.4$ in a non-magnetized plasma (Spitzer 1962). We do not consider the effects of turbulence on this reduction factor.

⁴There is some ambiguity in the right-hand side of equation (2). We take D and D_0 to be diffusion coefficients for particles of a specified energy as opposed to diffusion coefficients of a particle that diffuses in energy as well as space. Thus, D/D_0 may scale differently for electrons of energies, e.g., $k_B T$ and $2k_B T$. In the static-field approximation this is not an issue since D/D_0 is the same for all energies of interest for cluster parameters. However, when we estimate the effects of turbulent resistivity, we pick a representative energy at which to evaluate D/D_0 as discussed in section 6.

Three previous studies (Jokipii 1973, Skilling, McIvor, & Holmes 1974, Narayan & Medvedev 2001) calculated $L_S(r_0)$ for strong turbulence assuming a power spectrum of magnetic fluctuations on scales ranging from l_B to a much smaller dissipation scale l_d , which is approximately the proton gyroradius ρ_i in galaxy clusters (Quataert 1998). Using different definitions of L_S , each study found that $L_S(r_0)$ is of order l_B in the small- (r_0/l_B) and small- l_d/l_B limits provided r_0 is not vastly smaller than l_d . Jokipii (1973) assumed an isotropic turbulent magnetic field and employed a stochastic model of field-line separation, which he solved using a Monte Carlo numerical method. Skilling et al (1974) assumed isotropic turbulence and introduced an approximate equation of the form $d\langle r \rangle/dz = F(\langle r \rangle)$ for the average separation r of a pair of field lines, with the function F estimated from the power spectrum of the turbulence. Narayan & Medvedev (2001) introduced a similar equation for the evolution of the mean square separation, $d\langle r^2 \rangle/dl = G(\langle r^2 \rangle)$, and estimated G using the Goldreich-Sridhar (1995) model of anisotropic MHD turbulence.

In this paper, we calculate L_S using three different methods. First, we consider an approximate model in which the separation r of a pair of field lines evolves stochastically and is described by the Fokker-Planck equation

$$\frac{\partial P}{\partial l} = -\frac{\partial}{\partial y} \left[\left(\frac{\langle \Delta y \rangle}{\Delta l} \right) P \right] + \frac{\partial^2}{\partial y^2} \left[\left(\frac{\langle (\Delta y)^2 \rangle}{2\Delta l} \right) P \right], \quad (4)$$

where $y = \ln(r/l_B)$, l is distance along the field in units of l_B , Δy is the increment to y after a field-line pair is followed a distance Δl along the field, $\langle \dots \rangle$ is an average over a large number of field-line pairs, and $P(y_1, l)dy$ is the probability that y is in the interval $(y_1, y_1 + dy)$ after a distance l along the field. Our model is similar to Jokipii's (1973), although we determine the functional form of $\langle \Delta y \rangle / \Delta l$ and $\langle (\Delta y)^2 \rangle / \Delta l$ using the Goldreich-Sridhar model of locally anisotropic MHD turbulence, and we solve the Fokker Planck equation analytically, which allows us to determine the functional dependence of L_S on turbulence parameters. If we evaluate the turbulence parameters in the model using data from direct numerical simulations, we find that $L_S(r_0) \rightarrow 4.5l_B$ as r_0 is decreased towards l_d in the large- l_B/l_d limit, and that $L_S(\rho_e) \simeq L_S(l_d)$.

Our second method for calculating $L_S(r_0)$ uses a numerical Monte Carlo model of field line separation in which each random step Δy is of order unity (the Fokker-Planck equation assumes infinitesimal Markovian steps). When the model parameters are evaluated using data from direct numerical simulations, the Monte Carlo model gives $L_S(\rho_e) \simeq 6.5l_B$ in the large- l_B/l_d limit.

Our third method for calculating $L_S(r_0)$ involves tracking field-line trajectories in direct numerical simulations of MHD turbulence with zero mean magnetic field. The results of our highest resolution simulations are consistent with the prediction of the theoretical studies that $L_S(r_0)$ approaches a value of order several l_B as r_0 is decreased towards l_d in the large- l_B/l_d limit. Extrapolating our numerical results to the large- l_B/l_d limit suggests that $L_S(\rho_e) \simeq 5 - 10l_B$ in clusters.

Field evolution and turbulent fluid motions increase electron (and ion) mobility, enhancing κ_T

to some degree. Turbulent diffusion in clusters has been studied by Cho et al (2003). In this paper we develop a phenomenology to describe the interplay between field evolution and single-electron motion under the questionable assumption that turbulent resistivity completely reconnects field lines on the time scale l_B/u , where u is the rms turbulent velocity. A similar assumption was explored by Gruzinov (2002). We find three limiting cases for the thermal conductivity. For typical cluster parameters and turbulent velocities (Churazov et al 2003) $\kappa_T \sim \sqrt{\kappa_S u l_B}$, a value that is somewhat larger than both the turbulent diffusivity $\sim u l_B$ for that cluster and the static-field estimate of $\kappa_S l_B / L_S \simeq 0.1 \kappa_S - 0.2 \kappa_S$. More work, however, is needed to clarify the role of turbulent resistivity before firm conclusions can be drawn about its effects on κ_T . Additional work is also needed to quantify factors of order unity that have been neglected in estimating κ_T both in the presence of efficient turbulent resistivity and in the static-field approximation.

The remainder of this paper is organized as follows. In section 2 we review the phenomenology of thermal conduction in static tangled magnetic fields. In section 3, we discuss the effects of magnetic mirrors and microturbulence on electron diffusion along field lines. We present our Fokker-Planck and Monte Carlo models of field-line separation in section 4. We compare these approximate theoretical models with results from direct numerical simulations in section 5. We estimate the effects of turbulent resistivity on κ_T in section 6 and summarize our conclusions in section 7. We present numerical simulations of field-line separation for different types of MHD turbulence in a companion paper (Maron, Chandran, & Blackman 2003). Table 1 defines some frequently used notation.

2. The phenomenology of thermal conduction in a static tangled magnetic field

We assume that the magnetic fluctuations possess an inertial range extending from an outer scale l_B to a much smaller inner scale l_d with the magnetic energy dominated by scales $\simeq l_B$. Except where specified, the discussion focuses on the case relevant for clusters in which the mean magnetic field is negligible.

A tangled magnetic field line is essentially a random-walk path through space. If a particle is tied to a single field line and travels a distance $l \gg l_B$ along the static magnetic field, it takes $\sim l/l_B$ random-walk steps of length $\sim l_B$, resulting in a mean-square three-dimensional displacement of

$$\langle (\Delta x)^2 \rangle = \alpha l_B l, \quad (5)$$

where α is a constant of order unity (values of α for the numerical simulations used in this paper are listed in table 2). When there is a mean field \mathbf{B}_0 comparable to the rms field, $\langle (\Delta x)^2 \rangle$ in equation (5) is interpreted as the mean-square displacement perpendicular to \mathbf{B}_0 . If the particle's

Notation	Meaning
l_B	dominant length scale of the magnetic field
l_d	magnetic dissipation scale
$\langle l \rangle$	average distance in units of l_B that a field-line pair must be followed before separating by a
$\langle l^2 \rangle$	average square of the distance in units of l_B^2 that a field-line pair must be followed before separatin
$L_S(r_0)$	$l_B \langle l^2 \rangle / \langle l \rangle$ —characteristic distance a pair of field lines separated by a distance r_0 must be followed be
ρ_e	electron gyroradius
κ_T	thermal conductivity
κ_S	Spitzer thermal conductivity in a non-magnetized plasma
D	3D single-electron diffusion coefficient
D_0	3D single-electron diffusion coefficient in a non-magnetized plasma
D_{\parallel}	diffusion coefficient for electron motion along the magnetic field
λ	thermal-electron Coulomb mean free path
u	rms turbulent velocity

Table 1: Definitions.

motion along the field is diffusive with diffusion coefficient D_{\parallel} , then

$$l \sim \sqrt{D_{\parallel} t}, \quad (6)$$

and (Rechester & Rosenbluth 1978, Krommes et al 1983)

$$\langle (\Delta x)^2 \rangle \propto t^{1/2}, \quad (7)$$

indicating subdiffusion: $D \equiv \lim_{t \rightarrow \infty} \langle (\Delta x)^2 \rangle / 6t \rightarrow 0$ (see also Qin et al 2002a,b). This process is called double diffusion: the particle diffuses along the field line, and the field line itself is a random-walk path through space.

The vanishing of D for a particle tied to a single field line can be understood by considering a particle starting out at point P in figure 1. If this particle moves one Coulomb mean free path λ along its field line F_1 towards point Q and then randomizes its velocity due to collisions, it has a $\sim 50\%$ chance of changing its direction of motion along the magnetic field and returning to its initial point P. In contrast, in a Markovian three dimensional random walk, the second step is uncorrelated from the first and there is a vanishing probability that a particle will return to its initial location. In a cluster, $\rho_e/l_B \simeq 10^{-15}$, and thus it is tempting to assume that electrons are tied to field lines. The importance of equation (7) is that any study that assumes that electrons are perfectly tied to field lines will conclude that $\kappa_T = D = 0$.

Of course, an electron is not tied to a single field line. As pointed out by Rechester & Rosenbluth (1978), small cross-field motions enhanced by the divergence of neighboring field lines leads to a non-zero D . This can be seen with the aid of figure 1. Suppose an electron starts out at

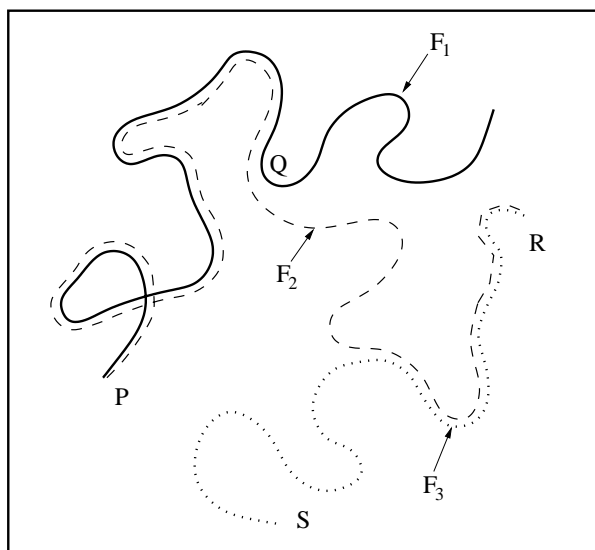


Fig. 1.— Trajectory of a diffusing electron.

point P on field line F_1 traveling towards point Q. After moving a short distance, field gradients and collisions cause the particle to take a step of length $\sim \rho_e$ across the magnetic field, from F_1 to a new field line F_2 . Although the electron continuously drifts across the field to new field lines, let us assume for the moment that it remains attached to F_2 . As the electron follows F_2 , F_2 diverges from F_1 . Let z be the distance that F_2 must be followed before F_2 separates from F_1 by a distance l_B . (Because the electron continuously drifts across the field, it typically separates from F_1 after traveling a distance somewhat less than z along the field; this effect, however, is ignored in this paper.) After the electron moves a distance z along F_2 , its subsequent motion is not correlated with F_1 . The electron proceeds to point R, and then its collisional random walk along the magnetic field changes direction, bringing it back towards point Q. Instead of following F_2 back to point Q, however, the electron drifts across the field and ends up on a new field line F_3 . After following F_3 for a distance $\sim z$, the electron separates from F_2 by a distance $\sim l_B$ and proceeds to point S.

In this example, the electron's small cross-field motions and the divergence of neighboring field lines allow the electron to escape from its initial field line and undergo a Markovian random walk in three dimensions. The fundamental random walk step is a displacement of length mz along the magnetic field, where m is some constant of order unity, perhaps 2 or 3. From equation (5),

when $mz \gg l_B$, a single random step corresponds to a 3D displacement of

$$(\Delta x)^2 \sim \alpha mz l_B. \quad (8)$$

[When $mz \gg l_B$, the difference between the actual value of $(\Delta x)^2$ and its mean becomes small.]
When $mz \gg \lambda$, where λ is the Coulomb mean free path, a single step takes a time

$$\Delta t \sim \frac{m^2 z^2}{D_{\parallel}}. \quad (9)$$

When mz is only moderately greater than l_B or λ , equations (8) and (9) remain approximately valid. During successive random steps, a particle will find itself in regions of differing magnetic shear, and thus z will vary. The diffusion coefficient is given by $D = \langle (\Delta x)^2 \rangle / 6 \langle \Delta t \rangle$ where $\langle \dots \rangle$ is an average over a large number of steps (Chandrasekhar 1943). Ignoring factors of order unity we obtain ⁵

$$D \sim \frac{D_{\parallel} l_B}{L_S}, \quad (10)$$

with

$$L_S = \frac{\langle z^2 \rangle}{\langle z \rangle}. \quad (11)$$

In general, L_S , $\langle z \rangle$, and $\langle z^2 \rangle$ are functions of the initial separation of a field-line pair, r_0 , but for electron thermal conduction we have set $r_0 = \rho_e$. If there is a mean magnetic field comparable to the fluctuating field, equation (10) is recovered provided D is replaced by D_{\perp} , the coefficient of diffusion perpendicular to the mean field. We note that taking $L_S = \langle z \rangle$ leads to similar results since $\langle z \rangle \sim \langle z^2 \rangle / \langle z \rangle$ in our direct numerical simulations and Fokker-Planck and Monte Carlo calculations. In clusters $D_{\parallel} \sim D_0$ as discussed in section 3, where D_0 is the electron diffusion coefficient in a non-magnetized plasma. As a result, equations (2) and (11) give

$$\kappa_T \simeq \frac{\kappa_S l_B}{L_S}. \quad (12)$$

3. Electron diffusion along the magnetic field

For mono-energetic electrons subject to a fixed Coulomb pitch-angle scattering frequency, the diffusion coefficient $D_{\parallel,0}$ for motion along a uniform magnetic field is equal to the three-dimensional diffusion coefficient D_0 for motion in a non-magnetized plasma. Two mechanisms

⁵In applying equation (8) first and then averaging z and z^2 , we are averaging separately over the wandering of a single field line through space and the separation of neighboring field lines. This is justified to some extent since the former is dominated by the value of \mathbf{B} at the outer scale and the latter depends on the magnetic shear throughout the inertial range. Although some error is introduced by averaging separately, equations (10) and (11) are sufficient for estimating κ_T .

for suppressing D_{\parallel} relative to $D_{\parallel,0}$ have been discussed in the literature: magnetic mirrors and wave pitch angle scattering. Magnetic mirrors associated with a cluster’s turbulent magnetic field significantly reduce D_{\parallel} only when $\lambda \gtrsim l_B$, where λ is the Coulomb mean free path of thermal electrons (Chandran & Cowley 1998, Malyshkin & Kulsrud 2001). In cluster cores, however, λ is significantly less than l_B , and thus mirrors have only a small effect. [For Hydra A and 3C295, $\lambda \sim 1$ kpc at 100 kpc from cluster center, and $\lambda = 0.02 - 0.05$ kpc at 10 kpc from cluster center (Narayan & Medvedev 2001).] When the Knudsen number $N_K \equiv \lambda/L_{T,\parallel}$ approaches 1, where $L_{T,\parallel} = T/|\hat{\mathbf{b}} \cdot \nabla T|$ and $\hat{\mathbf{b}}$ is a unit vector pointing along the magnetic field, the heat flux becomes large and excites whistler waves that enhance the pitch-angle scattering of electrons and reduce D_{\parallel} (Pistinner & Eichler 1998)⁶. However, for heat conduction into a cluster core, $|\nabla T| \sim T/R_c$ with $R_c \sim 100$ kpc, and $N_K \ll 1$. Thus, wave pitch-angle scattering has only a small effect, and

$$D_{\parallel} \sim D_0. \quad (13)$$

We note that the chaotic trajectories of field lines cause $L_{T,\parallel}$ to be larger than $T/|\nabla T|$.

4. Fokker-Planck and Monte Carlo models of field-line separation in strong MHD turbulence

We adopt the Goldreich & Sridhar (1995) model of strong locally anisotropic MHD turbulence, which is supported by direct numerical simulations (Cho & Vishniac 2000, Maron & Goldreich 2001, Cho & Lazarian 2003). We assume that the fluctuating field is equal to or greater than any mean field in the system. The separation of neighboring magnetic field lines in strong MHD turbulence is dominated by shear Alfvén modes. On scales smaller than l_B , an Alfvén-mode eddy is elongated along the direction of the average of the magnetic field within the volume of the eddy, denoted $\mathbf{B}_{\text{local}}$, with (Goldreich & Sridhar 1995, Cho & Vishniac 2000, Maron & Goldreich 2001, Lithwick & Goldreich 2001)

$$B_{\lambda_{\perp}} \sim B_{\text{local}} \left(\frac{\lambda_{\perp}}{l_B} \right)^{1/3}, \quad (14)$$

and

$$\lambda_{\parallel} \sim \lambda_{\perp}^{2/3} l_B^{1/3}, \quad (15)$$

where $B_{\lambda_{\perp}}$ is the rms magnetic fluctuation of an Alfvén-mode eddy of width λ_{\perp} measured across $\mathbf{B}_{\text{local}}$ and length λ_{\parallel} measured along $\mathbf{B}_{\text{local}}$. In fully ionized plasmas, the dissipation scale l_d for Alfvén modes is set by collisionless effects, and is comparable to the proton gyroradius ρ_i

⁶The formula in Pistinner & Eichler’s (1998) paper is $\kappa_T/\kappa_S \sim 1/[1 + 250\beta_e(\lambda/L_{T,\parallel})]$, but the factor of 250 should be corrected to a factor of 10 (Pistinner, private communication)

(Quataert 1998). The magnetic-field perturbation of an Alfvén mode is perpendicular to $\mathbf{B}_{\text{local}}$. Equations (14) and (15) thus imply that when two field lines separated by a distance r are followed for a distance $r^{2/3}l_B^{1/3}$, r either increases or decreases by a factor of order unity assuming $l_d < r < l_B$ (Narayan & Medvedev 2001, Maron & Goldreich 2001, Lithwick & Goldreich 2001). If $r < l_d$, the separation or convergence of the field lines is dominated by the eddies of width l_d , and r increases or decreases by a factor of order unity when the field lines are followed a distance $l_d^{2/3}l_B^{1/3}$ (Narayan & Medvedev 2001). We define

$$\Delta l = \begin{cases} (r/l_B)^{2/3} & \text{if } l_d < r < l_B \\ (l_d/l_B)^{2/3} & \text{if } r < l_d \end{cases}, \quad (16)$$

$$y = \ln(r/l_B), \quad (17)$$

Δy to be the change in y when the field lines are followed a distance Δl ,

$$a = \langle \Delta y \rangle, \quad (18)$$

with a taken to be positive, and

$$b = \langle (\Delta y)^2 \rangle / 2, \quad (19)$$

where a and b are of order unity.

To obtain Monte Carlo and analytic solutions for L_S , we make several approximations. The changes in r over a distance $r^{2/3}l_B^{1/3}$ along the field associated with eddies of width much smaller or larger than r (or l_d if $r < l_d$) are small compared to the changes arising from eddies of width r (or l_d if $r < l_d$) and are neglected. We also take a and b to be independent of l and y , and consecutive values of Δy to be uncorrelated. To obtain an approximate analytic solution for L_S , we make the further approximation of describing the stochastic variation of y with the Fokker-Planck equation

$$\frac{\partial P}{\partial l} = -\frac{\partial}{\partial y} \left[\left(\frac{\langle \Delta y \rangle}{\Delta l} \right) P \right] + \frac{\partial^2}{\partial y^2} \left[\left(\frac{\langle (\Delta y)^2 \rangle}{2\Delta l} \right) P \right], \quad (20)$$

where $P(y', l)dy$ is the probability that y is in the interval $(y', y' + dy)$, and l is distance along the magnetic field in units of l_B . The additional approximation in introducing equation (20) is associated with y changing by order unity during a single random step [equation (20) assumes infinitesimal steps].

We now solve equation (20) to obtain an analytic solution for L_S . Substituting equations (16), (18), and (19) into equation (20) yields

$$\frac{\partial P}{\partial l} = -\frac{\partial \Gamma}{\partial y}, \quad (21)$$

where

$$\Gamma = \begin{cases} ae^{-2y/3}P - \frac{\partial}{\partial y} \left(be^{-2y/3}P \right) & \text{if } y_d < y < 0 \\ ae^{-2y_d/3}P - be^{-2y_d/3} \frac{\partial P}{\partial y} & \text{if } y < y_d \end{cases}, \quad (22)$$

is the probability flux, and

$$y_d = \ln \left(\frac{d}{l_B} \right), \quad (23)$$

which is the value of y at the dissipation scale. We solve equation (21) with initial condition $P(y) = \delta(y - y_0)$ at $l = 0$ and boundary conditions $P = 0$ at $y = 0$, $P \rightarrow 0$ as $y \rightarrow -\infty$, and P and Γ continuous at $y = y_d$. For electron thermal conduction in galaxy clusters, the quantity of interest is L_S when the initial separation r_0 is the electron gyroradius, and thus we take $y_0 < y_d$. The boundary condition $P = 0$ at $y = 0$ means that $\Gamma(l, y = 0)dl$ gives the probability that a field-line pair separates to a distance l_B for the first time after a distance between l and $l + dl$ along the field.

We proceed by making the substitution

$$P = x^m f, \quad (24)$$

with

$$x = e^{y/3} \quad (25)$$

and

$$m = 2 + 3a/2b. \quad (26)$$

We then take the Laplace transform of equation (21), with the Laplace transform of f defined by

$$\bar{f}(s) = \int_0^\infty f(l) e^{-sl} dl. \quad (27)$$

For $x_d < x < 1$, where $x_d = e^{y_d/3}$ is the value of x at the dissipation scale,

$$\frac{\partial^2 \bar{f}}{\partial x^2} + \frac{1}{x} \frac{\partial \bar{f}}{\partial x} - \left(\frac{v^2}{x^2} + \frac{9s}{b} \right) \bar{f} = 0, \quad (28)$$

with

$$v = \frac{3a}{2b}. \quad (29)$$

Since $f(1) = 0$,

$$\bar{f} = c_1 [I_v(\psi x) K_v(\psi) - K_v(\psi x) I_v(\psi)], \quad (30)$$

where I_v and K_v are modified Bessel's functions,

$$\psi = 3 \sqrt{\frac{s}{b}}, \quad (31)$$

and c_1 is a constant to be determined by applying the boundary conditions at x_d after the solution for \bar{f} for $x < x_d$ has been obtained.

For $x < x_d$,

$$\frac{\partial^2 \bar{f}}{\partial x^2} + \frac{5}{x} \frac{\partial \bar{f}}{\partial x} + \frac{(4 - v^2 - \chi)\bar{f}}{x^2} = -\frac{3x_d^2 x_0^{-m-1} \delta(x - x_0)}{b}, \quad (32)$$

where

$$\chi = \frac{9x_d^2 s}{b} \quad (33)$$

and

$$x_0 = e^{y_0/3}. \quad (34)$$

For $x < x_0$,

$$\bar{f} = c_2 x^{-2+\sqrt{v^2+\chi}} + c_3 x^{-2-\sqrt{v^2+\chi}}. \quad (35)$$

For $x_0 < x < x_d$,

$$\bar{f} = c_4 x^{-2+\sqrt{v^2+\chi}} + c_5 x^{-2-\sqrt{v^2+\chi}}. \quad (36)$$

For $Re(s) \geq 0$, the boundary condition at $y = -\infty$ implies that $c_3 = 0$. Integrating equation (32) from $x_0 - \varepsilon$ to $x_0 + \varepsilon$ yields the jump condition for $\partial \bar{f} / \partial x$ at $x = x_0$. After applying this jump condition and the continuity of f and Γ at $x = x_d$, we find that

$$c_1 = \frac{3x_0^{-v+\sqrt{v^2+\chi}} x_d^{-\sqrt{v^2+\chi}}}{b(hT - \psi x_d U)}, \quad (37)$$

where

$$T = I_v(\psi x_d) K_v(\psi) - K_v(\psi x_d) I_v(\psi), \quad (38)$$

and

$$U = I'_v(\psi x_d) K_v(\psi) - K'_v(\psi x_d) I_v(\psi). \quad (39)$$

Since $I'_v(\psi) K_v(\psi) - K'_v(\psi) I_v(\psi) = 1/\psi$, we find that

$$\bar{\Gamma}(x=1) = -\frac{bc_1}{3}. \quad (40)$$

Since

$$\langle l^n \rangle = \int_0^\infty dl l^n \Gamma \Big|_{x=1} = \left(\frac{\partial}{\partial s} \right)^n \bar{\Gamma} \Big|_{x=1, s=0}, \quad (41)$$

where n is a non-negative integer, we have

$$\langle l^n \rangle = -\frac{b}{3} \frac{\partial^n c_1}{\partial s^n} \Big|_{s=0}. \quad (42)$$

Thus,

$$\langle l \rangle = \frac{9}{b} \left[\frac{1}{4(\nu+1)} + \frac{x_d^2}{2\nu} \ln \left(\frac{x_d}{x_0} \right) - \frac{x_d^2}{4\nu^2} \left(\nu - 1 + \frac{x_d^{2\nu}}{\nu+1} \right) \right]. \quad (43)$$

For fixed positive a in the limit $x_d \rightarrow 0$, equation (43) gives

$$\langle l \rangle = \frac{9}{2(2b+3a)}. \quad (44)$$

The full equation for $\langle l^2 \rangle$ is very long and will not be quoted here. However, for fixed positive a in the limit $x_d \rightarrow 0$, we find that

$$\langle l^2 \rangle = \frac{81(3a+6b)}{4(3a+2b)^2(3a+4b)}, \quad (45)$$

with $L_S/l_B = \langle l^2 \rangle / \langle l \rangle$ given by

$$\frac{L_S}{l_B} = \frac{9(3a+6b)}{2(3a+2b)(3a+4b)}. \quad (46)$$

From equation (43) $\langle l \rangle$ diverges for fixed x_d as $a \rightarrow 0$ (i.e. $\nu \rightarrow 0$).

We now check the analytic results with a Monte Carlo solution of equation (20) with initial conditions $P(y, l=0) = \delta(y - y_0)$, and with $y_0 = -10$ and $y_d = -8$. The Monte Carlo solution consists of iteratively incrementing a pair of numbers (l, y) . During each step, we increase l by an amount $\delta l = e^{2y/3} \varphi$ (or $\delta l = e^{2y_d/3} \varphi$ if $y < y_d$) and increase y by an amount $\delta y = a\varphi \pm k$, where the \pm sign is determined randomly with equal chance for either sign, and φ is a constant. As $\varphi \rightarrow 0$, each step becomes infinitesimal as is assumed in the Fokker-Planck equation. The value of k is chosen so that $\langle (\delta y)^2 \rangle = 2b\varphi$ (i.e., $k = \sqrt{2b\varphi - a^2\varphi^2}$). We stop incrementing l and y once y reaches 0, and record the value of l at the final step. We repeat this for 2000 ordered pairs to obtain $\langle l \rangle$ and $\langle l^2 \rangle$. The results of this procedure with $\varphi = 10^{-4}$ and $a = 0.3$ for various values of b are shown in figure 2, along with the analytic results of equations (44) and (45). We also plot Monte Carlo results with $\varphi = 1$, which provide a measure of the error associated with using a Fokker-Planck equation to describe the discrete stochastic process described by equations (16), (18), and (19).

In figure 3 we plot Monte Carlo calculations of $\langle l \rangle$ as a function of initial field-line separation r_0 for $b = 0.17$, $l_B/l_d = 50$, $\varphi = 10^{-4}$, and two values of a : $a = 0.01$ (solid triangles) and $a = 0.29$ (open triangles). The solid line is a plot of equation (44) for $a = 0.01$, and the dashed line is a plot of equation (44) for $a = 0.29$. The figure shows the increase in $\langle l \rangle$ as $a \rightarrow 0$ for fixed x_d .

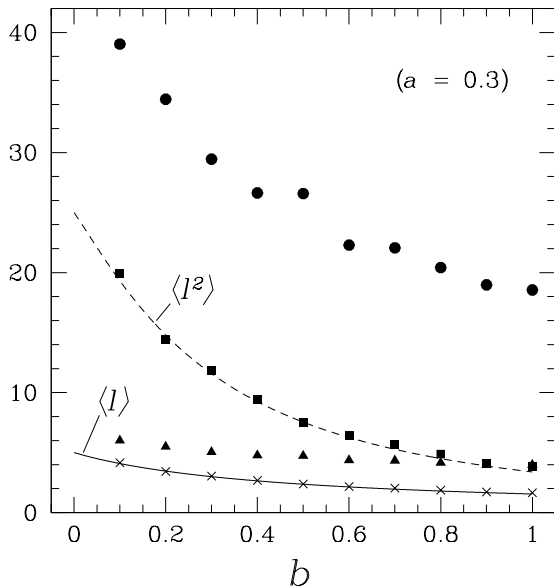


Fig. 2.— The solid line gives $\langle l \rangle$ from equation (44). The dashed line gives $\langle l^2 \rangle$ from equation (45). The \times s and squares give the values of $\langle l \rangle$ and $\langle l^2 \rangle$ from Monte Carlo calculations with $\phi = 10^{-4}$. The triangles and circles give the values of $\langle l \rangle$ and $\langle l^2 \rangle$ from Monte Carlo calculations with $\phi = 1$. For all data in plot, $a = 0.3$.

5. Direct numerical simulations

In this section, we study field-line separation in a static magnetic field using data obtained from direct numerical simulations of MHD turbulence. Galaxy clusters have very small mean magnetic fields, little rotation and thus little helicity, and very large magnetic Prandtl number P_m , where $P_m = \nu/\eta$, ν is the viscosity,⁷ and η is the resistivity. Ideally, we would like to generate cluster-like magnetic fields self-consistently within a direct numerical simulation. However, at present it is not clear how to do this. Numerical simulations of turbulent dynamos in high- P_m plasmas driven by non-helical forcing find that amplified magnetic fields remain concentrated on very small (resistive) spatial scales (Maron & Cowley 2001). Yet the Faraday rotation produced by intracluster plasmas indicates that clusters possess considerable amounts of magnetic energy on large scales of order 1 – 10 kpc. We are thus faced with several alternatives. We can choose a numerical model that matches the helicity, mean magnetic field, and magnetic Prandtl number conditions of clusters, in which case the spatial scale of the model magnetic field is far too small. Or we can choose a numerical model that produces a large-scale field by, for example, including

⁷For clusters with anisotropic plasma viscosity, ν is taken to be the parallel viscosity.

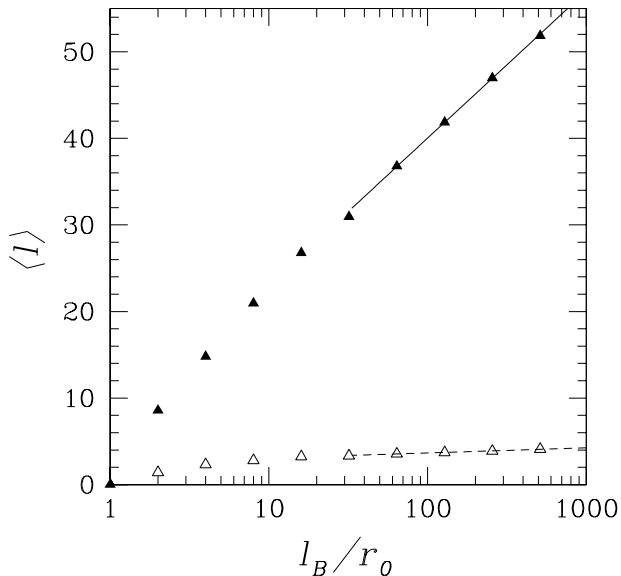


Fig. 3.— Monte Carlo calculations of $\langle l \rangle$ with $b = 0.17$, $l_B/l_d = 50$, $\phi = 10^{-4}$ and two values of a : $a = 0.01$ (solid triangles) and $a = 0.29$ (open triangles). The solid line is the analytic result [equation (43)] with $a = 0.01$, and the dashed line is the analytic result with $a = 0.29$.

a mean magnetic field, using helical forcing, or choosing initial conditions that ensure that the magnetic field remains large-scale.⁸

In this paper, we follow the latter course. We initialize a simulation with a random-phase magnetic field containing some amount of magnetic helicity, as well as random velocities with kinetic energies comparable to the magnetic energy. We allow the system to decay, leaving behind a large-scale magnetic field, which contains 10% of the maximum magnetic helicity for that magnetic energy. We then force the system non-helically at wavenumbers between $2\pi/L_{\text{box}}$ and $4\pi/L_{\text{box}}$, where L_{box}^3 is the volume of the simulation cube. The forcing sustains a Kolmogorov-like spectrum of magnetic and kinetic energy. The result is a turbulent magnetic field that is dominated by large-

⁸Haugen et al (2003) found that non-helical dynamos with P_m up to 30 result in a magnetic power spectrum $E_b(k)$ proportional to k^{-1} . Such a spectrum is neither large-scale-dominated nor small-scale-dominated, since each logarithmic interval of order unity in k -space contains the same amount of energy. However, they suggest that when both the ordinary Reynolds number R and P_m are large, there is a $k^{-5/3}$ spectrum at large scales followed by a k^{-1} spectrum at smaller scales, with the magnetic energy dominated by large-scale fluctuations. If this suggestion is correct, a very-high-resolution non-helical dynamo simulation with large R and large P_m would be a self-consistent way to generate a large-scale magnetic field in cluster-like conditions. Such a simulation, however, would be beyond our current computational resources.

scale fluctuations, has a Kolmogorov-like inertial range extending to small scales, has zero mean, and has relatively little magnetic helicity, which we take to be a reasonable model for magnetic fields in clusters. We carry out a first simulation (simulation A1) on 256^3 grid points, and then use A1 as an initial condition for a higher resolution version (simulation A2) on 512^3 grid points with reduced resistivity and viscosity. We use incompressible simulations, which are a reasonable approximation for subsonic turbulence in clusters. The simulations are three-dimensional and periodic, and the pseudo-spectral numerical method is described by Maron & Goldreich (2001). We use Newtonian viscosity and resistivity with $P_m = 1$, since simulating $P_m \gg 1$ in our isotropic-viscosity simulations requires a large viscosity that damps small-scale Alfvén waves; small-scale Alfvénic turbulence is present in clusters due to anisotropic plasma viscosity (Goldreich & Sridhar 1995, Quataert 1998), and plays an important role in field-line separation. In a companion paper, Maron, Chandran, & Blackman (2003), we study field-line separation in numerical simulations of different types of MHD turbulence and dynamo-generated fields.

The simulation parameters for A1 and A2 are summarized in table 1. In figure 4 we plot time averages of the magnetic power spectrum $E_b(k)$ [the total magnetic energy is $\int E_b(k)dk$], the kinetic power spectrum $E_v(k)$ [the total kinetic energy is $\int E_v(k)dk$], and the total-energy spectrum $E_{\text{total}}(k) = E_v(k) + E_b(k)$ in simulation A2. We set π/l_B equal to the maximum of $kE_b(k)$, giving $l_B = 0.25L_{\text{box}}$, and we set π/l_d equal to the maximum of $k^3E_b(k)$.

Simulation	Grid points	$ \langle \mathbf{B} \rangle $	H_m	l_B/l_d	α	$P_m = \nu/\eta$
A1	256^3	0	0.1	23	2.4	1
A2	512^3	0	0.1	50	2.4	1

Table 2: $|\langle \mathbf{B} \rangle|$ is the strength of the mean magnetic field, H_m is the magnetic helicity divided by the maximum possible magnetic helicity at that level of magnetic energy, l_B/l_d is the ratio of outer scale to inner scale, α is the single-field-line diffusion coefficient in equation (5), and $P_m = \nu/\eta$ is the magnetic Prandtl number, where ν and η are the viscosity and resistivity.

We run each simulation until the power spectrum reaches a statistical steady state before we start analyzing field lines. For simulation A1, we take seventeen snapshots of the magnetic field separated in time by an interval $0.4l_B/u$, where u is the rms turbulent velocity. To calculate L_S and $\langle l \rangle$ for an initial field-line separation r_0 , we introduce into each snapshot of the magnetic field 2,000 pairs of field-line tracers whose initial separation vector \mathbf{r}_0 is perpendicular to the local field. We use linear interpolation to obtain the magnetic field between grid points, employ second-order Runge-Kutta to integrate field-lines, and iteratively reduce the length step in the field-line integrations to achieve convergence. For simulation A2, we carry out the same procedure, but we use five snapshots of the magnetic field separated in time by an interval $0.2l_B/u$, and we use 20,000 pairs of field-line tracers per snapshot.

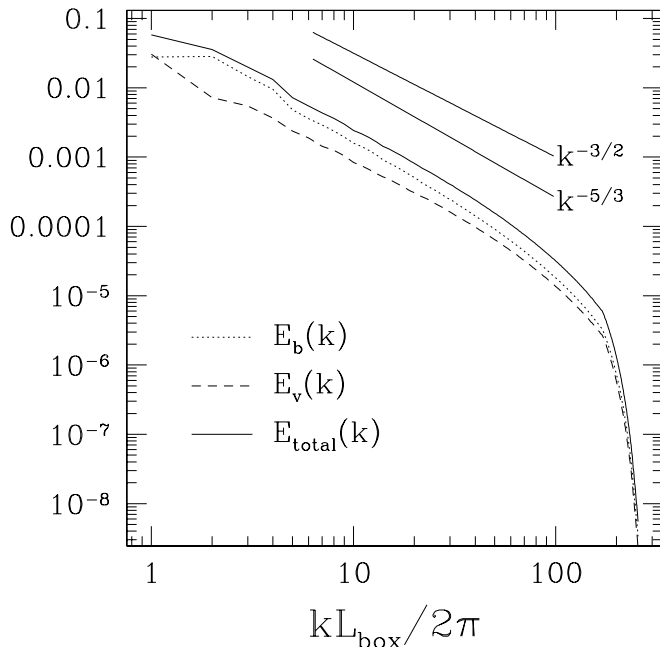


Fig. 4.— Power spectra in simulation A2. The dotted line is the magnetic power spectrum $E_b(k)$, the dashed line is the kinetic power spectrum $E_v(k)$, and the solid line is the total-energy spectrum $E_{\text{total}} = E_v(k) + E_b(k)$.

We first seek to test the qualitative prediction of the Fokker-Planck model and previous theoretical treatments (Jokipii 1973, Skilling et al 1974, Narayan & Medvedev 2001) that $\langle l \rangle$ and L_S/l_B asymptote to a constant of order a few as r_0 is decreased towards l_d in the large- l_B/l_d limit. In figure 5, we plot $\langle l \rangle$ for simulation A1 and simulation A2. The lower-resolution data of simulation A1 suggest the scaling $\langle l \rangle \propto \ln(l_B/r_0)$ for $l_d < r_0 < 0.25l_B$, in contradiction to the theoretical treatments. On the other hand, for simulation A2, the curve through the data is concave downward for $l_d < r_0 < l_B$. Moreover, figure 5 shows that the simulation A1 data, and probably also the A2 data, have not converged to the high-Reynolds-number values of $\langle l \rangle$ for $l_B/16 < r_0 < l_B$, values of r_0 that are within the inertial ranges (l_d to l_B) of both simulations. Also, the slope $d\langle l \rangle/d(\ln(l_B/r_0))$ for both $r_0 < l_d$ and $r_0 < l_B/10$ decreases significantly when l_B/l_d is doubled. A comparison of the data for A1 and A2 thus suggests that in the large- l_B/l_d limit $\langle l \rangle$ asymptotes to a value of order several l_B as r_0 is decreased towards l_d , as in the Fokker-Planck model and previous studies. The same comments apply to the data for L_S , which are plotted in figure 6.

Because the definition of l_B is not unique, we recalculate $\langle l \rangle$ and L_S , setting $2\pi/l_B$ equal to the maximum of $kE_b(k)$, so that l_B is twice its former value. Note that this affects both the unit for measuring distance along the field and also the distance to which field lines must separate. We plot the results in figures 7 and 8, which are qualitatively similar to the results based on our original

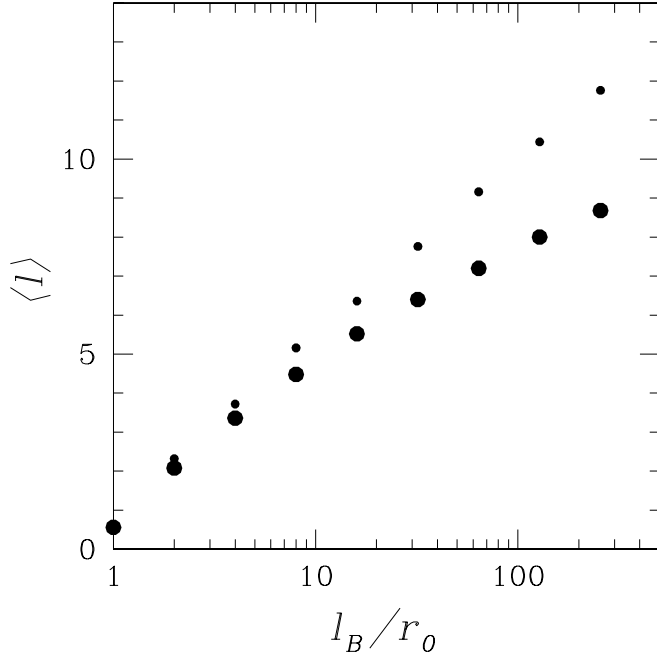


Fig. 5.— The average distance in units of l_B that a field-line pair must be followed before separating by a distance l_B , denoted $\langle l \rangle$, as a function of initial field-line separation r_0 for simulations A1 (small circles) and A2 (large circles).

definition of l_B .

We note that for $r_0 = l_B$, $\langle l \rangle$ and L_S are by definition 0. The numerical-simulation data points that appear to be plotted above $l_B/r_0 = 1$ actually correspond to r_0 just slightly smaller than l_B , indicating that $\langle l \rangle$ and L_S are discontinuous at $r_0 = l_B$ in the numerical simulations. The reason is that for r_0 just slightly less than l_B , some fraction of the field line pairs are initially converging and must be followed a significant distance before they start to diverge.

We evaluate characteristic values of a and b , defined in equations (18) and (19), in simulation A2 by calculating the mean and mean-square increments to $y = \ln(r/l_B)$ for field-line pairs initially separated by a distance $l_B/8$ during a displacement of $l_B/4$ along the magnetic field, using our original definition of l_B [$\pi/l_B = \text{maximum of } kE_b(k)$]. We find that $a = 0.29$ and $b = 0.17$. These values are used to obtain the Fokker-Planck results plotted in figure 9. The Monte Carlo results in figure 9 use the same values of a and b and employ many small random steps ($\varphi = 10^{-4}$), and are thus expected to reproduce the Fokker-Planck results. We also plot $\langle l \rangle$ for a random-phase version of A2, which is obtained by assigning each Fourier mode in simulation A2 a random phase without changing the modes' amplitudes. The figure shows that $\langle l \rangle$ is moderately larger in the direct numerical simulations than in both the random-phase data and the Fokker-Planck

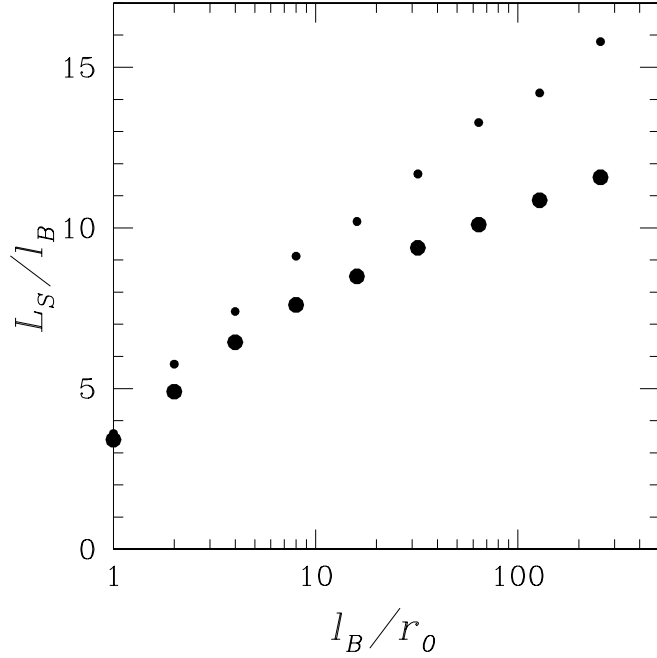


Fig. 6.— Value of L_S as a function of initial field-line separation r_0 in simulations A1 (small circles) and A2 (large circles).

model. If we take $a = 0.29$, $b = 0.17$, $l_d = \rho_i = 43\rho_e$, and $l_B/l_d \gg 1$, the Fokker-Planck model yields $L_S(\rho_e) \simeq L_S(l_d) \simeq 4.5l_B$ and the Monte Carlo model with order-unity random increments to $\ln(r/l_B)$ (i.e. $\phi = 1$) yields $L_S(\rho_e) \simeq L_S(l_d) \simeq 6.5l_B$.

In figure 10 we plot the probability distribution of the distance in units of l_B that a pair of field lines in simulation A2 with initial separation $r_0 = l_d$ must be followed before the field lines separate by a distance l_B . We define the function $\text{PDF}(l)$ so that the probability that l lies in some interval is proportional to the corresponding area under the plotted curve.

For clusters, $l_B/l_d \simeq l_B/\rho_i \simeq 10^{13}$. In the large- l_B/l_d limit, the numerical simulations and theoretical models indicate that L_S asymptotes to a value of order several l_B as r_0 is decreased towards l_d , and L_S is not expected to increase appreciably as r_0 is further decreased from $l_d = \rho_i$ to ρ_e . Thus, $L_S(\rho_e) \simeq L_S(l_d)$. To estimate $L_S(l_d)$ in clusters, we note that $L_S(l_d) \simeq 11l_B$ in simulation A1, and $L_S(l_d) \simeq 10l_B$ in simulation A2. When the definition of l_B is changed as in figure 8, so that $2\pi/l_B$ corresponds to the maximum of $kE_b(k)$, then $L_S(l_d) \simeq 7l_B$ in simulation A1 and $L_S(l_d) \simeq 6.5l_B$ in simulation A2. As mentioned previously, it is not clear which definition of l_B leads to a more accurate prediction of κ_T . We conclude from the direct numerical simulations suggest that $L_S(\rho_e) \simeq L_S(l_d) \simeq 5 - 10l_B$ in the large- l_B/l_d limit.

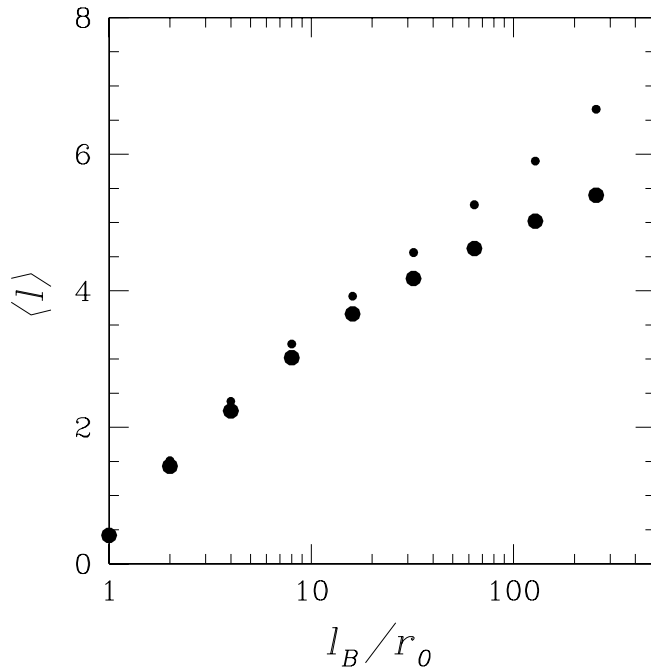


Fig. 7.— The average distance in units of l_B that a field-line pair must be followed before separating by a distance l_B as a function of initial field-line separation r_0 for simulations A1 and A2 (small and large solid circles). Same as figure 5, except that l_B is redefined to be twice as large.

6. Thermal conduction in time-varying turbulent magnetic fields

In this section, we develop a phenomenology of particle diffusion in time-varying turbulent magnetic fields under the questionable assumption that the magnetic field is completely randomized and reconnected on the eddy turnover time τ at scale l_B , $\tau = l_B/u$, where u is the rms velocity and the velocity outer scale l_0 is assumed equal to l_B . A similar assumption was explored by Gruzinov (2002). For simplicity, we assume that the magnetic-field randomization occurs instantaneously at regular time intervals of duration τ . We assume $\tau \gg \lambda/v_{te}$, where v_{te} is the electron thermal velocity and λ is the Coulomb mean free path, so that particle motion along the field over a time interval τ is diffusive. We assume that $\lambda \ll L_S$, so that particle motion along the field over a distance L_S is diffusive. We also assume that $v_{te} \gg u$.

There are three limiting cases. First, if $\tau \gg L_S^2/D_{\parallel}$, a particle escapes its initial field line through parallel motion and slow cross-field diffusion before the field is randomized. The “fundamental random-walk step” is of length L_S along the field, as in section 2, and takes a time L_S^2/D_{\parallel} . There are $n_{\text{steps}} = \tau D_{\parallel}/L_S^2$ such steps during each time interval τ . The three dimensional distance travelled by an electron along the magnetic field during one “fundamental random-walk step” is $\sim \sqrt{L_S l_B}$, and the three-dimensional distance travelled during n_{steps} steps is $\sim \sqrt{n_{\text{steps}} L_S l_B}$. On

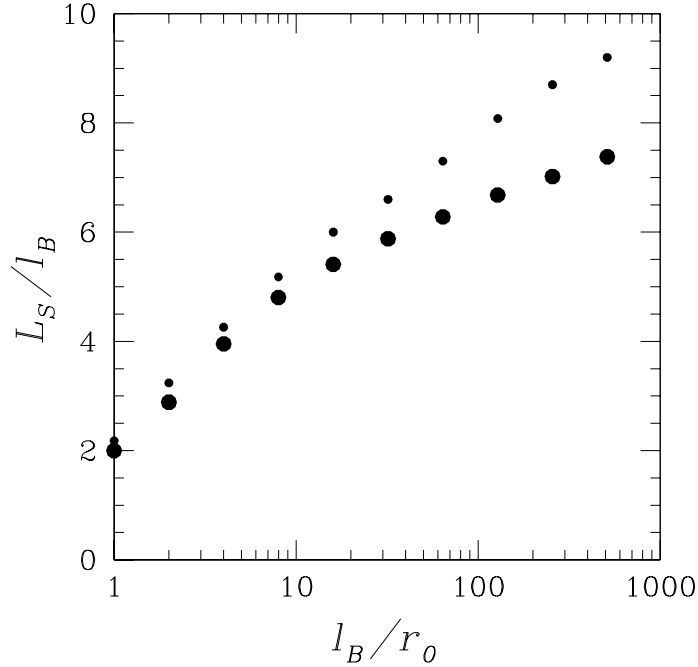


Fig. 8.— Value of L_S as a function of initial field-line separation r_0 in simulations A1 (small circles) and A2 (large circles). Same as figure 6, except that l_B is redefined to be twice as large.

the other hand, a fluid element travels a distance l_B during a time τ . Since $L_S > l_B$ and $n_{\text{steps}} \gg 1$, the distance travelled by a single electron during a time τ is much greater than the distance travelled by a fluid element, and the fluid motion can be ignored. The electron diffusion coefficient is then the same as in the static-field case.

At the other extreme is the limit $\tau \ll l_B^2/D_{\parallel}$. Since $l_B < L_S$, a particle escapes a field line through field-line randomization before it escapes through parallel motion and slow cross-field diffusion, and the fundamental random-walk step is of duration τ . The distance an electron travels along the field due to parallel diffusion, $\sqrt{D_{\parallel}\tau}$, is less than the distance l_B that a fluid element travels. The net displacement of an electron (or ion) during one fundamental random step, denoted Δr , is then given by

$$\Delta r \sim l_B. \quad (47)$$

Since the field is completely randomized after a time τ , magnetic tension does not inhibit the wandering of fluid parcels over times $\gg \tau$, as in Vainshtein & Rosner (1991) and Cattaneo (1994). Successive random steps are thus uncorrelated, giving a diffusion coefficient $\Delta r^2/\tau \sim l_B^2/\tau = ul_B$, as in hydrodynamical turbulent diffusion. In this limit, the parallel diffusion of electrons plays no role.

The third and intermediate case is $l_B^2/D_{\parallel} \ll \tau \ll L_S^2/D_{\parallel}$. In this case, the field is again random-

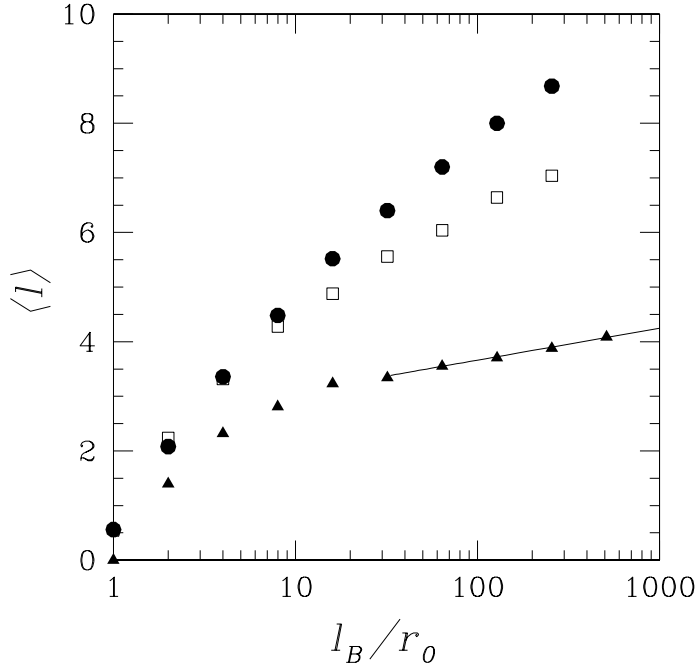


Fig. 9.— The average distance in units of l_B that a field-line pair must be followed before separating by a distance l_B as a function of initial field-line separation r_0 for simulation A2 (solid circles), the random-phase version of A2 (open squares), Monte Carlo simulations with $\phi = 10^{-4}$ (solid triangles), and the analytic Fokker-Planck model (solid line). The Monte Carlo and Fokker-Planck solutions use $a = 0.29$, $b = 0.17$, and $l_B/l_d = 50$, values corresponding to simulation A2.

ized before a particle can escape its initial field line through parallel motion and slow cross-field diffusion, and the fundamental random-walk step is of duration τ . During one such step, a particle moves an rms distance $\sim \sqrt{D_{\parallel}\tau}$ along the field, which corresponds to an rms three dimensional displacement

$$\Delta r \sim (l_B \sqrt{D_{\parallel}\tau})^{1/2}. \quad (48)$$

The diffusion coefficient $\Delta r^2/\tau$ is then

$$D \sim \sqrt{D_{\parallel} u l_B}. \quad (49)$$

As an example, we consider the cluster A1795 at a distance of 100 kpc from cluster center, with an electron density of 0.01 cm^{-3} and a temperature of 5 keV (Ettori et al 2002). We consider slightly superthermal electrons with $D_{\parallel} = \kappa_S = 10^{31} \text{ cm}^2/\text{s}$. Churazov et al (2003) find evidence for turbulent velocities of order one-half the sound speed in the hot intracluster plasma of the Perseus cluster, which we take to be typical of A1795 as well, giving $u \simeq 350 \text{ km/s}$. We also assume $l_B = 10 \text{ kpc}$ at this distance from cluster center, and take $L_S = 6l_B$. For these parameters,

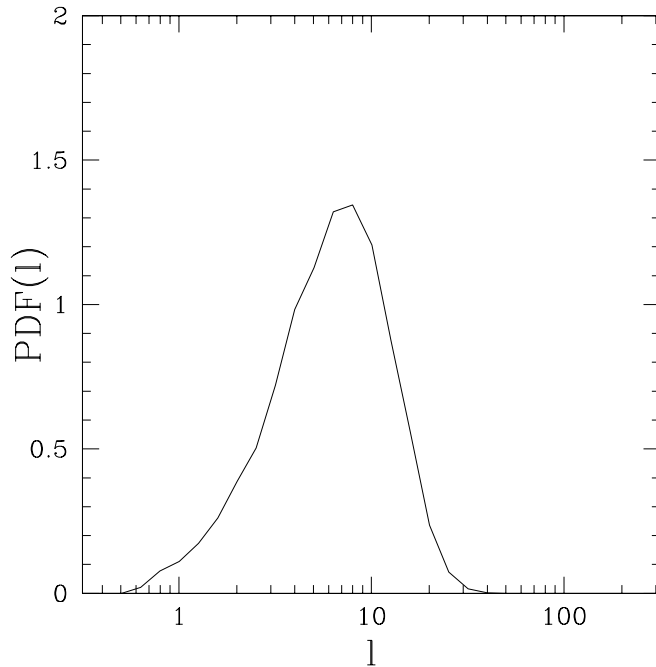


Fig. 10.— Probability distribution of the distance (in units of l_B) a field-line pair in simulation A2 initially separated by a distance l_d must be followed before separating by a distance l_B .

the plasma satisfies $l_B^2/D_{\parallel} < \tau < L_S^2/D_{\parallel}$. Equations (2), (13), and (49) then give

$$\kappa_T \sim \sqrt{\kappa_S u l_B}, \tag{50}$$

which is about $0.3\kappa_S$, or $3ul_B$. This value is roughly twice the estimate $\kappa_S l_B/L_S$, but given the uncertainties in both estimates, and the untested assumption that field lines are completely randomized and reconnected on the time scale τ , it is not clear that turbulent resistivity in fact enhances the thermal conductivity in clusters.

7. Summary

In this paper we consider the effects of field-line tangling and turbulent resistivity on the thermal conductivity κ_T in galaxy clusters. In the static-magnetic-field approximation, tangled field lines force electrons to move greater distances in traveling from hotter regions to colder regions, reducing κ_T by a factor of $\sim 5 - 10$ relative to the Spitzer thermal conductivity κ_S of a non-magnetized plasma for typical cluster parameters. It is possible that turbulent resistivity enhances κ_T by a moderate amount relative to the static-field estimate for typical cluster conditions, but further work is needed to investigate this possibility.

We thank Eric Blackman, Steve Cowley, and Alex Schekochihin for valuable discussions. This work was supported by NSF grant AST-0098086 and DOE grants DE-FG02-01ER54658 and DE-FC02-01ER54651 at the University of Iowa, with computing resources provided by the National Partnership for Advanced Computational Infrastructure and the National Center for Supercomputing Applications.

Allen, S., Taylor, G., Nulsen, P., Johnstone, R., David, L., Etori, S., Fabian, A., Forman, W., Jones, C., & McNamara, B. 2001, *MNRAS*, 324, 842

Binney, J., & Cowie, L. 1981, *ApJ*, 247, 464

Binney, J., & Tabor, G. 1995, *MNRAS*, 276, 663

Bohringer, H., & Morfill, G. E. 1988, *ApJ*, 330, 609

Bregman, J., & David, L. 1989, *ApJ*, 341, 49

Cattaneo, F. 1994, *ApJ*, 434, 200

Chandran, B. 1997, *ApJ*, 485, 148

Chandran, B. 2003, *ApJ*, submitted

Chandran, B., & Cowley, S. 1998, *Phys. Rev. Lett.*, 80, 3077

Chandran, B., & Rodriguez, O. 1997, *ApJ*, 490, 156

Chandrasekhar, S. 1943, *Rev. Mod. Phys.*, 15, 1

Cho, J., & Lazarian, A., 2003 *Phys. Rev. Lett.* in press

Cho, J., Lazarian, A., Honein, A., Knaepen, B., Kassinos, S., and Moin P. 2003, *ApJ*, submitted

Cho, J., & Vishniac, E. 2000, *ApJ*, 539, 273

Chun, E., & Rosner, R. 1993, *ApJ*, 408

Churazov, E., Forman, W., Jones, C., Sunyaev, R., & Bohringer, H. 2003, *MNRAS*, accepted for publication

Ciotti, L., & Ostriker, J. 2001, *ApJ*, 551, 131

Churazov, E., Sunyaev, R., Forman, W., & Bohringer, H. 2002, *MNRAS*, 332, 729

Crawford, C., Allen, S., Ebeling, H., Edge, A., Fabian, A. 1999, *MNRAS*, 306, 875

Etori, S., Fabian, A., Allen, S., & Johnstone, R. 2002, *MNRAS*, 331, 635

- Fabian, A. C. 1994, *Ann. Rev. Astr. Astrophys.*, 32, 277
- Fabian, A. C. 2002, astro-ph/0210150
- Goldreich, P. & Sridhar, S. 1995, *ApJ*, 438, 763
- Gruzinov, A. 2002, astro-ph/0203031
- Krommes, J., Oberman, C., & Kleva, R. 1983, *J. Plasma Phys.*, 30, 11
- Jokipii, J. 1973, *ApJ*, 183, 1029
- Lithwick, Y., & Goldreich, P. 2001, *ApJ*, 562, 279
- Loewenstein, M., & Fabian, A. 1990, *MNRAS*, 242, 120
- Malyshkin, L., & Kulsrud, R. 2001, *ApJ*, 549, 402
- Maron, J., Chandran, B., & Blackman, E. 2003, in preparation
- Maron, J., & Cowley, S. 2001, astro-ph/0111008
- Maron, J., & Goldreich, P. 2001, *ApJ*, 554, 1175
- Maron, J., & Blackman, E. 2002, *ApJ*, 566, L41
- Narayan, R., & Medvedev, M. 2001, *ApJ*, 562, 129
- Pedlar, A., Ghataure, H. S., Davies, R. C., Harrison, B. A., Perley, R., Crane, P. C., & Unger, S. W. 1990, *MNRAS*, 246, 477
- Perley, R., Taylor, G. 1991, *AJ*, 101, 1623
- Peterson, J. A. et al 2001, *A&A*, 365, L104
- Pistinner, S., & Eichler, D. 1998, *MNRAS*, 301, 49
- Qin, G., Matthaeus, W., & Bieber, J. 2002a, *ApJ*, 578, L117
- Qin, G., Matthaeus, W., & Bieber, J. 2002b, *Geophys. Res. Lett.* 29, 7
- Quataert, E. 1998, *ApJ*, 500, 978
- Rechester, R., & Rosenbluth, M. 1978, *Phys. Rev. Lett.*, 40, 38
- Rosner, R., & Tucker, W. 1989, *ApJ*, 338, 761
- Skilling, J., McIvor, I., & Holmes, J. 1974, *MNRAS*, 167, 87P
- Tabor, G., & Binney, J. 1993, *MNRAS*, 263, 323

- Tamura, T. et al 2001, A&A, 365, L87
- Tao, L. 1995, MNRAS, 275, 965
- Taylor, G., Fabian, A., Allen, S. 2002, MNRAS, 334, 769
- Taylor, G., Govoni, F., Allen, S., Fabian, A. 2001, MNRAS, 326, 2
- Tribble, P. 1989, MNRAS, 238, 1247
- Tucker, W. H., & Rosner, R. 1983, ApJ, 267, 547
- Vainshtein, S., & Rosner, R. 1991, ApJ, 376, 199
- Voigt, L. M., Schmidt, R. W., Fabian, A. C., Allen, S. W., & Johnstone, R. M. 2002, *Mon. Not. R. Astr. Soc.*, submitted (astro-ph/0203312)
- Zakamska, N., & Narayan, R. 2003, ApJ, in press